

# Experimental realization of a quantum game on a one-way quantum computer

Robert Prevedel<sup>1</sup>, André Stefanov<sup>1,2</sup>, Philip Walther<sup>3</sup> and Anton Zeilinger<sup>1,2</sup>

**Abstract.** We report the first demonstration of a quantum game on an all-optical one-way quantum computer. Following a recent theoretical proposal we implement a quantum version of Prisoner's Dilemma, where the quantum circuit is realized by a 4-qubit box-cluster configuration and the player's local strategies by measurements performed on the physical qubits of the cluster. This demonstration underlines the strength and versatility of the one-way model and we expect that this will trigger further interest in designing quantum protocols and algorithms to be tested in state-of-the-art cluster resources.

<sup>1</sup>Faculty of Physics, University of Vienna, Boltzmannngasse 5, A-1090 Vienna, Austria

<sup>2</sup>Institute for Quantum Optics and Quantum Information (IQOQI), Austrian Academy of Sciences, Boltzmannngasse 3, A-1090 Vienna, Austria

<sup>3</sup>Physics Department, Harvard University, Cambridge, Massachusetts 02138, USA

E-mail: [zeilinger-office@quantum.at](mailto:zeilinger-office@quantum.at)

PACS numbers: 03.67.-a, 03.67.Lx, 02.50.Le

## 1. Introduction

In the past, classical game theory has been extensively used to study problems such as stock market development, human as well as animal behavior or even the evolution of viruses at the microbiological level [1, 2, 3]. Quantum versions [4, 5, 6] of existing games offer additional strategies to the players - and resolve dilemmas that occur in the classical versions. As it is possible to recast any algorithm (classical or quantum) as a game characterized by strategies and rules, it is reasonable to believe that the quantum mechanical formulation of existing games can also be helpful in gathering a deeper understanding of quantum algorithms and quantum information processing. It has even been argued that performing experiments in physics can be viewed as simply playing a “game” against nature in which the observer tries to maximize the information obtained from the system under consideration. Eventually, such studies may even shed light on the great divide between classical and quantum physics [7].

The Prisoner’s Dilemma is a widely known example in classical game theory. It is a two players non-zero sum game where the players may benefit from unknowing cooperation. Due to the interesting nature of the game and the fact that communication is forbidden, defection turns out to be the unilateral best strategy, making it a *Nash*-equilibrium [1]. The dilemma arises because this strategy does not provide both players with the collective best payoff (which would be cooperation). However, extending the game into the quantum domain resolves the dilemma, as was first pointed out by Eisert *et al.* [5]. In the quantum version of the game, entanglement introduces some sort of cooperativity between the players and changes the Nash-equilibrium, so that the collective best choice for both players and the best individual choices are equal.

The quantum version of the Prisoner’s Dilemma has recently been experimentally demonstrated using a nuclear magnetic resonance (NMR) quantum computer [8]. Here we present the first optical implementation within the one-way model of quantum computation. By employing an all-optical system where the qubits are encoded in the polarization degree of freedom of the photons, the quantum states are subject to negligible decoherence and can easily be distributed among distant players. Moreover, in stark contrast to NMR quantum computing [9], in an all-optical implementation the observed entanglement can always be described as pure - and since the introduction of entanglement gives rise to the interesting features of quantum games we consider it important to report on an experimental realization which is free of any ambiguity in this respect.

Our implementation of the quantum version of the Prisoner’s Dilemma follows a recent proposal [10] which uses optical cluster states to realize the quantum game’s circuit. Since cluster states are the resource states for one-way quantum computing [11, 12, 13, 14], our demonstration is equivalent to playing the game on a quantum computer. The choice of a photonic system guarantees the externally-controlled implementation of the player’s strategy to a high degree. Additionally, the underlying principles of one-way quantum computing along with demonstrations of simple quantum

algorithms [15, 16, 17] as well as the generation of cluster states [18, 19, 20] have recently been successfully demonstrated using linear optics.

The subsequent parts of the paper are structured as follows. A brief explanation of the Prisoner’s Dilemma in the classical as well as in the quantum domain is given in Section 2. A succinct introduction into the paradigm of one-way quantum computing and the formulation of the game in its context follows in Section 3. The description of our experimental demonstration as well as the results of our investigation can be found in Section 4 while the concluding discussion is in Section 5.

## 2. The Prisoner’s Dilemma

The Prisoner’s Dilemma is a non zero-sum two players game. In the classical version, each player  $j \in \{A, B\}$  independently chooses a strategy  $s_j$  which is a binary choice  $s_j \in \{d, c\}$ . The choices are sent to a supervising referee who computes the payoff of each player  $\$_j(s_A, s_B)$  according to a payoff table. Since both players aim to maximize their individual payoff, the game is known to have a non-cooperative and selfish character.

The payoff table for player A is shown in Table 1 and as it is a symmetric game, player B’s payoffs are given by the transposed table. With the strategy profile  $(d, d)$  neither player can increase his/her individual payoff regardless of the opposition, making it a *Nash equilibrium* [1]. However the cooperative profile  $s = (c, c)$  is *Pareto-optimal* [2] since no player can increase their payoff by changing strategy, without reducing the payoff of the opponent. Classically, the Dilemma arises since  $(d, d)$  is a dominant profile (rational reasoning causes both players to choose this strategy) but the associated payoff is not the overall best available to them.

A\B	$c$	$d$
$c$	$\$_A(c, c) = 3$	$\$_A(c, d) = 0$
$d$	$\$_A(d, c) = 5$	$\$_A(d, d) = 1$

**Table 1.** Payoff table of player A for the classical Prisoner’s Dilemma. Since this is a symmetric game, player B’s payoffs are given by the transposed table.

In the quantum version of this game, however, this dilemma can be solved. Introducing entanglement provides both players with the ability to cooperate and therefore with an increased strategy space, effectively changing the Nash-equilibrium [5]. Suppose the strategy is realized by qubits, on which each player can perform their strategy by applying unitary operations. Following [5], the new strategy space is spanned by the unitary operator

$$U_j(\theta_j, \phi_j) = \begin{pmatrix} e^{-i\phi_j} \cos(\theta_j/2) & -\sin(\theta_j/2) \\ \sin(\theta_j/2) & e^{i\phi_j} \cos(\theta_j/2) \end{pmatrix}, \tag{1}$$

where  $\theta \in [0, \pi]$  and  $\phi \in [0, \pi/2]$ . The respective classical strategies  $c$  and  $d$  are realized by  $U_j(0, 0)$  and  $U_j(\pi, 0)$ . Before and after the operation of the players, the two qubits

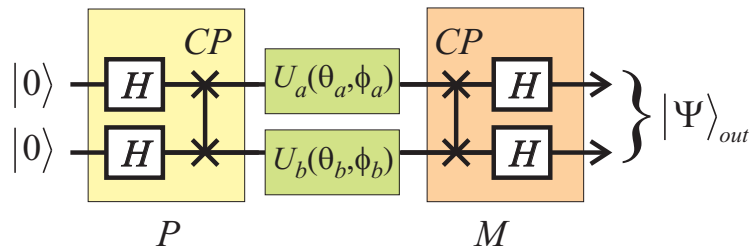


**Figure 1.** Quantum circuit of a two player quantum game,  $H$  is a Hadamard gate and  $CP$  a CPhase gate. The output state of the circuit is sent to a referee who computes the payoffs.

are subjected to entangling operations denoted  $P$  and  $M$  (see Fig. 1), which in our specific game, are a combination of Hadamard and CPhase ( $CP$ ) operations (a CPhase operation is a two-qubit entangling gate, which in the logical basis adds a  $\Pi$  phase shift to the  $|11\rangle$  term). Without those entangling steps the quantum version would not differ from a probabilistic, classic game. The corresponding quantum circuit is shown in Fig. 1. To compute the payoffs in the quantum version the referee projects the two qubit state onto the computational basis  $\{|0\rangle, |1\rangle\}$  and distributes the payoff according to the payoff table.

Depending on the player's actual choice of strategy (i.e. the unitary  $U_j$ ), the cooperativity due to the shared entanglement is preserved, giving rise to a Pareto optimal point that coincides with the Nash-equilibrium.

### 3. Playing the game on a one-way quantum computer

The entangling stages ( $P$  and  $M$ ) that are introduced in the quantum version of the game can be engineered by two-qubit gates. Two-qubit gates are crucial elementary gates for quantum computation [21] and have recently been demonstrated in the all-optical regime [22, 23, 24, 25, 26, 27]. In the one-way model of computation, such gates can be implemented by a proper measurement pattern on a sufficiently large entangled resource state (cluster state) [13, 15]. A specific way to implement the Prisoner's Dilemma on an all-optical one-way quantum computer was proposed by Paternostro *et al.* [10]. The main advantage of the one-way model is that the entangling gates are already intrinsically implemented in the structure of the cluster state, such that the actual game can easily be carried out by single-qubit rotations only. We will briefly discuss this in the following.

In the alternative and elegant model of one-way quantum computing the information processing is achieved by performing single-qubit measurements on a highly-entangled multi-particle cluster state [13]. This shifts the difficulty of realizing unitary gates to the generation of an appropriately designed multi-particle entangled state - often called cluster state - which serves as a resource for the computation. The processing of information is accomplished by sequential single-qubit measurements on the cluster qubits, greatly facilitating the computation itself. Given a cluster state, measurements

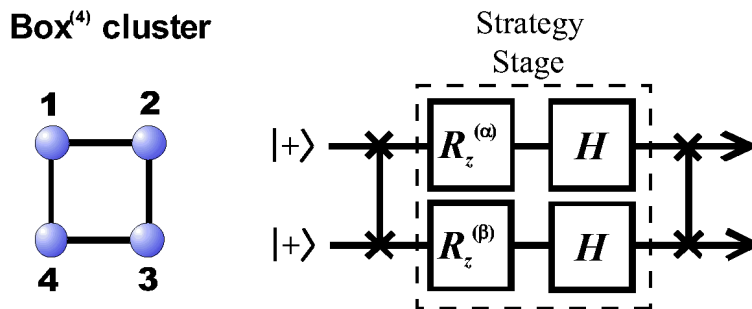


**Figure 2.** Left: Schematic representation of a box-cluster state. Physical qubits (blue spheres) are entangled to their nearest neighbors (indicated by a black line) by applying CPhase gates between them. Right: The quantum circuit realized by the box-cluster state. Note that the input states are initialized as the logical  $|+\rangle$  state, which is equivalent to a Hadamard gate acting on the  $|0\rangle$  state. Therefore the box-cluster implements, up to single-qubit rotations, the desired quantum circuit depicted in Fig. 1.

in the computational basis  $\{|0\rangle, |1\rangle\}$  have the effects of disentangling the qubit, while leaving the remaining qubits entangled. Measurements performed in a different basis denoted  $\{|\alpha_+\rangle, |\alpha_-\rangle\}$ , where  $|\alpha_\pm\rangle = (|0\rangle \pm e^{i\alpha}|1\rangle)/\sqrt{2}$ , also effectively rotate the logical qubit that undergoes the computation. In our case, the rotation is around the z-axis  $R_z(\alpha) = \exp(i\alpha\sigma_z/2)$  and followed by a Hadamard gate  $H$ . Rotations around the x-axis, i.e.  $R_x(\alpha) = \exp(i\alpha\sigma_x/2)$  can be implemented through the matrix identity  $R_x(\alpha) = HR_z(\alpha)H$ . An elaborated and detailed introduction to experimental one-way quantum computing is discussed in [15, 16]. Any complex operation (consisting of one- and two-qubit gates) can be carried out by a suitable choice of measurement patterns on a sufficiently large cluster state, so that, literally, the specific sequence of measurements forms the algorithms that is computed.

A special cluster state configuration, the box-cluster, is depicted in Fig. 2. It allows the implementation of a given set of unitaries  $U_j$  on two logical qubits as defined in the quantum circuit in Fig. 1, by measurement of qubits 1 and 4 in appropriate basis. This processes the input states, which are initialized as the logical  $|+\rangle$  states, and transfers them across the cluster to qubits 2 and 3. During this process, which is often referred to as *one-bit teleportation*, the logical qubit undergoes the unitary  $U_j$ , depending on the measurement basis and its outcome.

However, closer investigation reveals that measurements performed in the  $\{|\alpha_+\rangle, |\alpha_-\rangle\}$  basis would only allow  $R_z(\alpha)H$  operations, which do not belong to the strategy space defined by Eq.(1) apart for  $\alpha = \pi/2$ , consequently limiting the strategy space to  $\{c, q\}$  where  $q = U_j(0, \pi/2)$ . Therefore we have to introduce an additional single-qubit rotation before the measurements, as described in [10]. Then the strategy space can be increased to  $\{c, d, q(\alpha)\}$  where  $q(\alpha) = U_j(0, \alpha)$ , which allows an experimental realization of the quantum version of the game, as will be discussed in the following section.

#### 4. Experimental Realization

The cluster state creation is based on a interferometric method employing entangled photon pairs produced by spontaneous parametric down-conversion [28] and was first demonstrated in Ref. [15]. An ultra-violet laser pulse (1 W, 150 fs,  $\lambda = 394.5$  nm) passes twice through a non-linear crystal (BBO), thereby generating polarization-entangled photon pairs in both the forward (modes  $a$  and  $b$ ) and backward (modes  $c$  and  $d$ ) direction (see Fig. 3). Half-wave plates (HWP) and BBO crystals are used to counteract walk-off effects in the down-conversion crystal [28]. They are aligned such that  $\Phi^-$  and  $\Phi^+$  states are emitted in the forward and backward direction, respectively. Taking into account the possibility of double-pair emission into each direction and the action of the polarizing beam splitters (PBS) mixing modes  $a - d$  and  $b - c$ , the four amplitudes of the cluster state can be generated by rotating an additional HWP in mode  $a$  (see Ref. [15] for further details). Subsequently, the photons pass narrowband interference filters ( $\delta\lambda = 3nm$ ), and are then coupled into single-mode fibres and guided to the detection stage, where the photon's polarization is detected in an arbitrary basis using a combination of quarter-wave plates (QWP), HWP and PBS (see Fig. 3). A multichannel coincidence unit allows simultaneous detection of all relevant 16 four-fold coincidence events, therefore significantly speeding up the tomography process. The relative phase between the forward and backward emission in the setup sets the phases of the four individual terms of the cluster state. In the experiment, this is achieved with a piezo actuator translating the pump mirror. In the experiment, generation of the cluster state is retrodictive: it is known to have been prepared when one photon in each output port of the PBS's is detected. This postselection technique is well established in linear optics and ensures that photon loss and photodetector inefficiency do not affect the experimental results.

In an ideal case, the following four-photon state is produced by the experimental set-up:

$$|\Phi_c\rangle = \frac{1}{2}(|0000\rangle + |0011\rangle + |1100\rangle - |1111\rangle)_{1234} \quad (2)$$

with  $|0\rangle_j$  ( $|1\rangle_j$ ) embodied by the horizontal (vertical) polarization state of one photon populating a spatial mode  $j = 1, \dots, 4$ . The state  $|\Phi_c\rangle$  can be converted to the box cluster state (Fig. 2) by the local unitary operation  $H_1 \otimes H_2 \otimes H_3 \otimes H_4$  and a swap (or relabeling) of qubits 2 and 3 [15].

The quality of the generated cluster state is quantified by performing full quantum state tomography [29]. The reconstructed density matrix of the experimentally produced state,  $\varrho$ , is presented in Fig. 3 and has a fidelity with the ideal state in Eq. (2) of  $F = \langle \Phi_c | \varrho | \Phi_c \rangle = 0.62 \pm 0.01$ . The error bar of this result was estimated by performing a 100 run Monte Carlo simulation of the whole state tomography analysis, with Poissonian noise added to the count statistics in each run [25]. Higher fidelities are difficult to achieve due to phase instability during the lengthy process of state tomography and non-ideal optical elements employed in the setup. However, it is well-above the limit

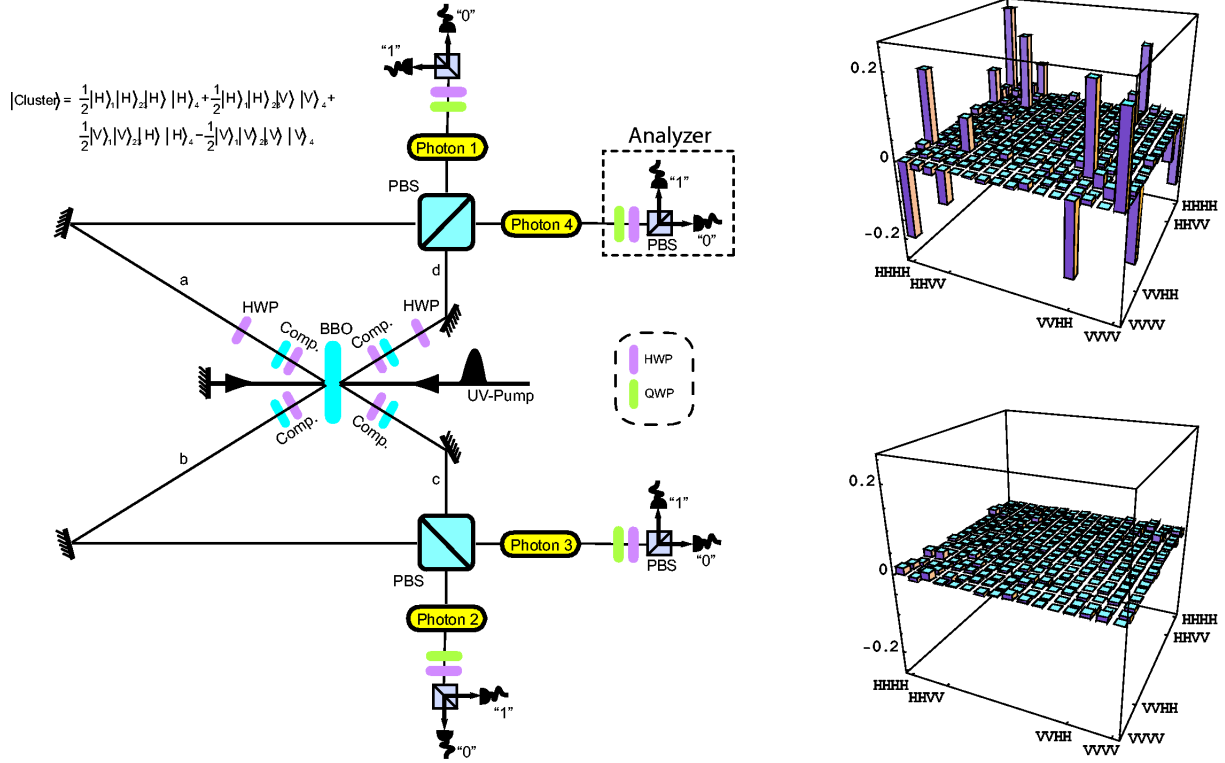


**Figure 3.** Left: Schematic drawing of the experimental setup that is employed to realize the quantum version of the Prisoner's Dilemma. Whenever one photon is emitted into each of the four output ports of the PBSs (mixing modes  $a - d$  and  $b - c$ ), a photonic 4-qubit cluster state is generated. The analyzers, which consist of QWP, HWP and PBS, allow measurements in an arbitrary polarization basis and therefore the implementation of the quantum game. Details are discussed in the text. Right: Tomographic plot of the generated cluster state with the real part (upper plot) and imaginary part (lower plot) of the density matrix.

$F = 0.5$  for any biseparable four-qubit state [30]. This demonstrates the presence of genuine four particle entanglement and confirms that such an experimental state can be used for the quantum protocol under consideration.

Starting from the state (2) the game is implemented by projecting the photons 1 and 4 onto the state  $|\theta_{1,4}\rangle_{1,4} = \cos(\theta_{1,4})|0\rangle_{1,4} + \sin(\theta_{1,4})|1\rangle_{1,4}$  resulting in the state  $|\psi(\theta_1; \theta_4)\rangle_{23} = {}_1\langle\theta|_4\langle\theta_4|\Phi_c\rangle_{1234}$  where  $\theta_1$  and  $\theta_4$  determine the strategies of players A and B, respectively, up to a rotation on the remaining photons. This projection in the laboratory basis is equivalent, up to a Hadamard rotation, to the box cluster state. The final state  $|\Psi\rangle_{23}^{out}$ , after the projection and any relevant  $\sigma_y$  operations are applied to them, resides on qubits 2 and 3 which are sent to the referee who calculates the payoff. The experimental parameters for the chosen strategies can be inferred from Table 2. In the appendix we give a detailed derivation of this table.

Experimentally the payoffs are determined as follows. We project the remaining two photons onto the  $\{|0\rangle, |1\rangle\}$  basis and measure the probabilities  $p_{ij} = |\langle ij | \Psi \rangle_{23}^{out}|^2$ .

A \ B	$c$	$d$	$q(\alpha_B)$
$c$	$\mathbb{I} \otimes \mathbb{I}  \psi(0; 0)\rangle$	$\sigma_y \otimes \mathbb{I}  \psi(0; -\pi/2)\rangle$	$\mathbb{I} \otimes \mathbb{I}  \psi(0; \alpha_B)\rangle$
$d$	$\mathbb{I} \otimes \sigma_y  \psi(-\pi/2; 0)\rangle$	$\sigma_y \otimes \sigma_y  \psi(-\pi/2; -\pi/2)\rangle$	$\mathbb{I} \otimes \sigma_y  \psi(-\pi/2; \alpha_B)\rangle$
$q(\alpha_A)$	$\mathbb{I} \otimes \mathbb{I}  \psi(\alpha_A; 0)\rangle$	$\sigma_y \otimes \mathbb{I}  \psi(\alpha_A; -\pi/2)\rangle$	$\mathbb{I} \otimes \mathbb{I}  \psi(\alpha_A; \alpha_B)\rangle$

**Table 2.** Table of the states after the players implemented their strategies.  $|\psi(\alpha_A, \alpha_B)\rangle$  is the state after both player applied their projections with angles  $\alpha_A$  and  $\alpha_B$  as described in the text. The final state  $|\Psi\rangle_{23}^{out}$  is obtained by applying an additional rotation  $\sigma_y$  if necessary.

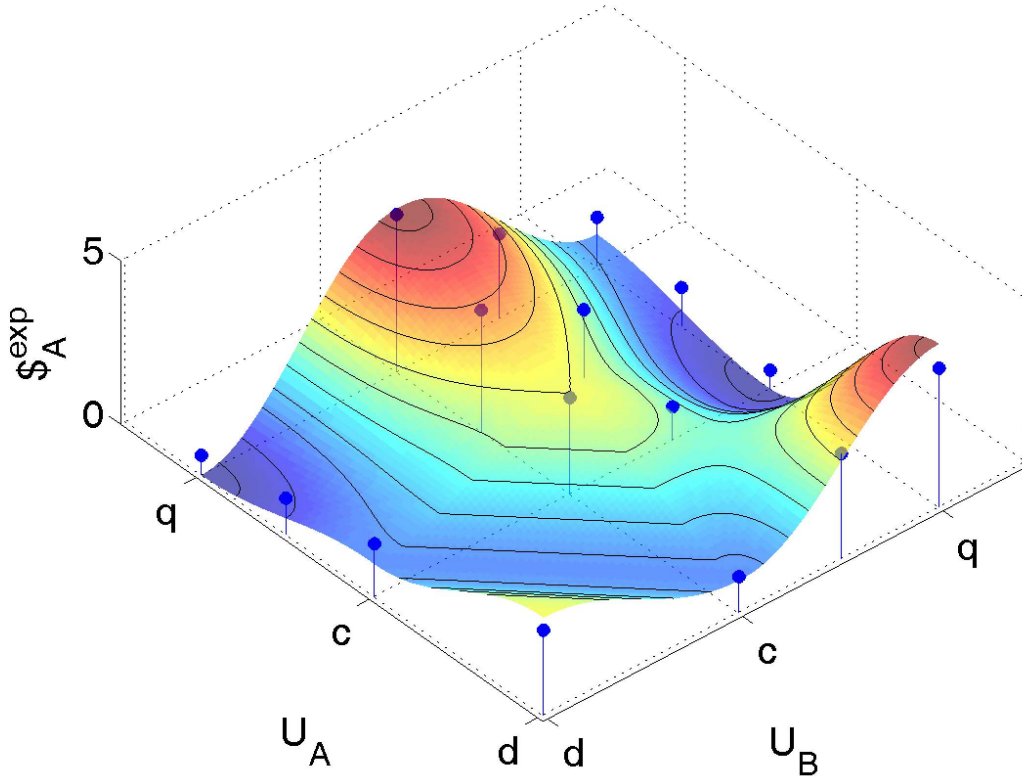


**Figure 4.** Graphical representation of the theoretical (surface) and measured (dots) payoffs of player A as a function of both players' strategies. The interval  $[d, c]$  is defined by the strategies  $U_j(\theta, 0)$  with  $\theta \in [\pi, 0]$  and  $[c, q]$  by the strategies  $U_j(0, \phi)$  with  $\phi \in [0, \pi/2]$ . The strategy profile  $(d, d)$  is Pareto-optimal and a Nash equilibrium thus resolving the dilemma occurring in the classical version of the game.

The payoff of player A is then computed using

$$\$_A^{\text{exp}}(s_A, s_B) = \$_A(c, c)p_{00} + \$_A(c, d)p_{01} + \$_A(d, c)p_{10} + \$_A(d, d)p_{11} \quad (3)$$

For each player we have chosen the following 4 strategies  $\{c, d, q(\pi/4), q(\pi/2)\}$ . Fig. 4 shows the experimental payoffs for all possible combinations of the implemented strategies. For comparison, the expected, ideal payoff function is also shown as a surface plot. We find good agreement between the measured and expected values.

The discrepancies are due to the non-ideal cluster state resource at hand. Unwanted correlations are known to affect the computation performed according to the one-way model in a protocol-dependent fashion [31]. Moreover, some of the payoffs corresponding to specific strategic moves played by A and B, suffer from the imperfect resource more than other, due to the specific nature of the measurement being performed. We emphasize that although we cannot implement  $U(\alpha, 0)$  strategies with arbitrary  $\alpha$ , our strategy space is still large enough to resolve the dilemma.

## 5. Discussion and outlook

We have experimentally demonstrated the application of a measurement-based protocol to realize a quantum version of the Prisoner’s Dilemma. Our implementation is based on entangled photonic cluster states and constitutes the first realization of a quantum game in the context of one-way quantum computing. Furthermore, our particular realization is especially suited for playing between distant parties. Because all the entangling operations preparing the cluster state are done locally by the referee, it is easy to distribute the entangled photons, even over large distances. Here we note that, of course, the game can also be played using an ancillary entangled pair for the realization of the disentangling CPhase gate. In this scenario, initially both players share one particle of an entangled photon pair and apply a polarization rotation on their respective photon  $U_j(\theta_j, \phi_j)$  (corresponding to their chosen strategy). The photons are then sent to the referee who applies the disentangling operation with an ancillary, entangled pair [23]. However such an operation experimentally requires interferometric stability between the initial and the ancilla pairs, a very difficult experimental challenge if the players reside at distant locations.

Another interesting feature is that, in our demonstration, the entanglement generation is decoupled from the actual processing of the quantum mechanical information. It remains an open question whether applications of few qubit cluster states could facilitate some kind of remote quantum information processing, e.g. multi-party quantum communication protocols [32]. Nonetheless, we also expect that the simple nature of our demonstration will trigger further interest in the one-way model of quantum computation, in particular in the realization of simple quantum algorithms.

## Acknowledgments

We want to thank M. Paternostro and M.S. Tame for fruitful discussions as well as A. Fedrizzi for careful reading of the manuscript. We acknowledge financial support by the FWF, the European Commission under the Integrated Project Qubit Applications (QAP) and the U.S. Army Research Office funded DTO (QCCM).

## Appendix

In order to find the correspondence between the quantum circuit which describes the game, as depicted in Fig. 1, and the sequence of measurements on the cluster state, we compare the output state of the circuit for each chosen strategy to the corresponding output state of the one-way computation sequence. The output state of the circuit for the input state  $|00\rangle$  is

$$|\Psi\rangle_{out} = [H \otimes H] \cdot CP \cdot [U_a(\theta_a, \phi_a) \otimes U_b(\theta_b, \phi_b)] \cdot CP \cdot [H \otimes H] |00\rangle$$

where the CPhase gate ( $CP$ ) is defined by

$$CP = \begin{pmatrix} 1 & 0 & 0 & 0 \\ 0 & 1 & 0 & 0 \\ 0 & 0 & 1 & 0 \\ 0 & 0 & 0 & -1 \end{pmatrix}.$$

Table A1 shows the output states as a function of the player's local strategies. Projecting these states onto the computational basis leads to the payoffs shown in Table A2. When the (dis)entangling operations are removed from the circuit this payoff table reduces to the original Table 1.

A \ B	$c$	$d$	$q(\alpha_B)$
$c$	$ 00\rangle$	$- 11\rangle$	$\cos(\alpha_B) 00\rangle - i \sin(\alpha_B) 01\rangle$
$d$	$- 11\rangle$	$- 00\rangle$	$i \sin(\alpha_B) 10\rangle - \cos(\alpha_B) 11\rangle$
$q(\alpha_A)$	$\cos(\alpha_A) 00\rangle$ $-i \sin(\alpha_A) 10\rangle$	$i \sin(\alpha_A) 01\rangle$ $-\cos(\alpha_A) 11\rangle$	$\cos(\alpha_A) \cos(\alpha_B) 00\rangle - i \cos(\alpha_A) \sin(\alpha_B) 01\rangle$ $-i \sin(\alpha_A) \cos(\alpha_B) 10\rangle - \sin(\alpha_A) \sin(\alpha_B) 11\rangle$

**Table A1.** Output states from the game circuit as a function of players' A and B strategies. Although these states are separable, they cannot be obtained by local unitary operations and without the action of (dis-)entangling operations between the players.

A \ B	$c$	$d$	$q(\alpha_B)$
$c$	$\$A(c, c)$	$\$A(d, d)$	$ \cos(\alpha_B) ^2 \$A(c, c) +  \sin(\alpha_B) ^2 \$A(c, d)$
$d$	$\$A(d, d)$	$\$A(c, c)$	$ \sin(\alpha_B) ^2 \$A(d, c) +  \cos(\alpha_B) ^2 \$A(d, d)$
$q(\alpha_A)$	$ \cos(\alpha_A) ^2 \$A(c, c)$ $+  \sin(\alpha_A) ^2 \$A(d, c)$	$ \sin(\alpha_A) ^2 \$A(c, d)$ $+  \cos(\alpha_A) ^2 \$A(d, d)$	$ \cos(\alpha_A) \cos(\alpha_B) ^2 \$A(c, c)$ $+  \cos(\alpha_A) \sin(\alpha_B) ^2 \$A(c, d)$ $+  \sin(\alpha_A) \cos(\alpha_B) ^2 \$A(d, c)$ $+  \sin(\alpha_A) \sin(\alpha_B) ^2 \$A(d, d)$

**Table A2.** Payoffs for player A computed using the states from Table A1.

Next we show how a cluster state can be used to simulate the quantum circuit corresponding to the quantum game. The cluster state  $|\Phi_c\rangle = \frac{1}{2}(|0000\rangle + |0011\rangle + |1100\rangle - |1111\rangle)_{1234}$  is projected onto a two photon state by projecting the qubit 1 and

4 onto the states  $\cos(\theta_{1,4})|0\rangle_{1,4} + e^{i\varphi_{1,4}}\sin(\theta_{1,4})|1\rangle_{1,4}$ . We verify that the remaining two-photon state is equivalent to the circuit outcome up to a local rotation on each remaining qubit. Before the rotation the state is

$$\begin{aligned} |\psi(\theta_1, \varphi_1; \theta_4, \varphi_4)\rangle_{23} &= \cos(\theta_1)\cos(\theta_4)|00\rangle_{23} + e^{i\varphi_4}\cos(\theta_1)\sin(\theta_4)|01\rangle_{23} \\ &+ e^{i\varphi_1}\sin(\theta_1)\cos(\theta_4)|10\rangle_{23} - e^{i(\varphi_1+\varphi_4)}\sin(\theta_1)\sin(\theta_4)|11\rangle_{23} \end{aligned}$$

When Player A and B apply a rotation  $R_j(\alpha_j, \beta_j, \gamma_j)$  on qubit 3 and qubit 2 respectively, the final output state is

$$|\Psi\rangle_{23}^{out} = R_B(\alpha_B, \beta_B, \gamma_B) \otimes R_A(\alpha_A, \beta_A, \gamma_A) |\psi(\theta_1, \varphi_1; \theta_4, \varphi_4)\rangle_{23}$$

where

$$R(\alpha, \beta, \gamma) = R_z(\alpha) R_x(\beta) R_z(\gamma) = \begin{pmatrix} e^{i(\alpha-\gamma)}\cos(\beta/2) & -e^{i(\alpha+\gamma)}\sin(\beta/2) \\ e^{i(\alpha-\gamma)}\sin(\beta/2) & e^{i(\alpha+\gamma)}\cos(\beta/2) \end{pmatrix}$$

Table A3 shows the final states as a function of the strategies. Although they are not strictly equal to the output of the quantum circuit, those states lead to the same payoffs when measured in the computational basis. This proves the equivalence of both approaches and shows that it is necessary, in order to span the entire strategy space, to extend the cluster state scheme by allowing arbitrary one-qubit rotations. However, we note that the strategies  $m = U(\alpha, 0)$  are not accessible because the output of the circuit for the strategy  $(s_A, s_B) = (q(\alpha), c)$  is  $\cos(\alpha/2)|00\rangle - \sin(\alpha/2)|11\rangle$ . Such an output cannot be achieved using a cluster state of the form of Eq. 2 for any  $\alpha$  different from 0 or  $\pi$ . A six photon cluster state [20] would be required to implement the whole space of strategies  $U_j(\theta_j, \phi_j)$ .

A \ B	$c$	$d$	$q(\alpha_B)$
$c$	$\mathbb{I} \otimes \mathbb{I}  \psi(0; 0)\rangle$	$-i\sigma_y \otimes \mathbb{I}  \psi(0; -\pi/2)\rangle$	$\mathbb{I} \otimes \mathbb{I}  \psi(0; \alpha_B)\rangle$
$d$	$-i \cdot \mathbb{I} \otimes \sigma_y  \psi(-\pi/2; 0)\rangle$	$-\sigma_y \otimes \sigma_y  \psi(-\pi/2; -\pi/2)\rangle$	$-\mathbb{I} \otimes i\sigma_y  \psi(-\pi/2; \alpha_B)\rangle$
$q(\alpha_A)$	$\mathbb{I} \otimes \mathbb{I}  \psi(\alpha_A; 0)\rangle$	$-i\sigma_y \otimes \mathbb{I}  \psi(\alpha_A; -\pi/2)\rangle$	$\mathbb{I} \otimes \mathbb{I}  \psi(\alpha_A; \alpha_B)\rangle$

**Table A3.** Table of the projected states and rotation angles corresponding to different strategies, with  $\mathbb{I} = R_j(0, 0, 0)$ ,  $-i\sigma_y = R_j(0, \pi, 0)$  and  $|\psi(\alpha_A; \alpha_B)\rangle = |\psi(\alpha_A, 0; \alpha_B, 0)\rangle_{23}$ .

## References

- [1] Myerson R B 1991 *Game Theory: An Analysis of Conflict* (MIT Press, Cambridge, MA)
- [2] Fudenberg D and Tirole J 1991 *Game Theory* (MIT Press)
- [3] Turner P E and Cho L 1999 *Nature* **398** 441
- [4] Meyer D A 1999 *Phys. Rev. Lett.* **82** 1052
- [5] Eisert J, Wilkens M and Lewenstein M 1999 *Phys. Rev. Lett.* **83** 3077
- [6] Benjamin S C and Hayden P M 2001 *Phys. Rev. A* **64** 030301

- [7] Lee C F and Johnson N F 2002 *Physics World* **15** 25
- [8] Du J, Li H, Xu X, Shi M, Wu J, Zhou X and Han R 2002 *Phys. Rev. Lett.* **88** 137902
- [9] Braunstein S L, Caves C M, Jozsa R, Linden N, Popescu S and Schack R 1999 *Phys. Rev. Lett.* **83** 1054
- [10] Paternostro M, Tame M S and Kim M S 2005 *New J. Phys.* **7** 226
- [11] Briegel H J and Raussendorf R 2001 *Phys. Rev. Lett.* **86** 910
- [12] Nielsen M A 2004 *Phys. Rev. Lett.* **93** 040503
- [13] Raussendorf R and Briegel H J 2001 *Phys. Rev. Lett.* **86** 5188
- [14] Raussendorf R, Browne D E and Briegel H J 2003 *Phys. Rev. A* **68** 2231201
- [15] Walther P, Resch K J, Rudolph T, Schenck E, Weinfurter H, Vedral V, Aspelmeyer M and Zeilinger A 2005 *Nature* **434** 169
- [16] Prevedel R, Walther P, Tiefenbacher F, Böhi P, Kaltenbaek R, Jennewein T and Zeilinger A 2007 *Nature* **445** 65
- [17] Tame M S, Prevedel R, Paternostro M, Böhi P, Kim M S and Zeilinger A 2007 *Phys. Rev. Lett.* **98** 140501
- [18] Kiesel N, Schmid C, Weber U, Tóth G, Gühne O, Ursin R and Weinfurter H 2005 *Phys. Rev. Lett.* **95** 210502
- [19] Zhang A N, Lu C Y, Zhou X Q, Chen Y A, Zhao Z, Yang T and Pan J W 2006 *Phys. Rev. A* **73** 022330
- [20] Lu C Y, Zhou X Q, Gühne O, Gao W B, Zhang J, Yuan Z S, Goebel A, Yang T and Pan J W 2007 *Nature Physics* **3** 91
- [21] Barenco A, Bennett C H, Cleve R, DiVincenzo D P, Margolu N, Shor P, Sleator T, Smolin J A and Weinfurter H 1995 *Phys. Rev. A* **52** 3457
- [22] O'Brien J L, Pryde G J, White A G, Ralph T C and Branning D 2003 *Nature* **426** 264
- [23] Gasparoni S, Pan J W, Walther P, Rudolph T and Zeilinger 2004 *Phys. Rev. Lett.* **93** 020504
- [24] Pittman T B, Fitch M J, Jacobs B C and Franson J D 2003 *Phys. Rev. A* **68** 32316
- [25] Langford N K, Weinhold T J, Prevedel R, Resch K J, Gilchrist A, O'Brien J L, Pryde G J and White A G 2005 *Phys. Rev. Lett.* **95** 210504
- [26] Kiesel N, Schmid C, Weber U, Ursin R and Weinfurter H 2005 *Phys. Rev. Lett.* **95** 210505
- [27] Okamoto R, Hofmann H, Takeuchi S and Sasaki K 2005 *Phys. Rev. Lett.* **95** 210506
- [28] Kwiat P G, Mattle K, Weinfurter H, Zeilinger A, Sergienk A V and Shih Y 1995 *Phys. Rev. Lett.* **75** 4337
- [29] James D F V, Kwiat P G, Munro W J and White A G 2001 *Phys. Rev. A* **64** 52312
- [30] Tóth G and Gühne O 2005 *Phys. Rev. Lett.* **94** 060501
- [31] Tame M S, Paternostro M, Kim M S and Vedral V 2006 *Phys. Rev. A* **73** 022309
- [32] Munro W J, Nemoto K and Spiller T P 2005 *New J. Phys.* **7** 137